Investigating orthogonal interactions between 20S proteasome subunits by humanizing assembly chaperones in *Saccharomyces cerevisiae*

Homin Jeong

A Thesis

in

The Department

of

Biology

Presented in Partial Fulfillment of the Requirements

for the Degree of Master of Science (Biology) at

Concordia University,

Montreal, Quebec, Canada

December 2024

CONCORDIA UNIVERSITY

School of Graduate Studies

This is to certify that the thesis prepared

By: Homin Jeong

Entitled: Investigating orthogonal interactions between 20S proteasome subunits by humanizing assembly chaperones in *Saccharomyces cerevisiae*

and submitted in partial fulfillment of the requirements for the degree of

Master of Science (Biology)

complies with the regulations of the University and meets the accepted standards with respect to originality and quality.

Signed by the final Examining Committee:

_____ External Examiner

Dr. William Zerges

_____ Examiner

Dr. Elena Kuzmin

_____ Examiner

Dr. David Kwan

_____ Supervisor

Dr. Christopher Brett

Approved by: _____

Graduate Program Director, Dr. Robert Weladji

_____

Dean of Faculty, Dr. Pascale Sicotte

_____ 2024

Abstract

Investigating orthogonal interactions between 20S proteasome subunits

by humanizing assembly chaperones in *Saccharomyces cerevisiae*

Homin Jeong

The proteasome is a large, multi-subunit protein complex essential for degrading unneeded, misfolded or damaged proteins in eukaryotic cells. Mutations in its subunits are linked to many human diseases. How these mutations affect proteasome function remains unclear, so scientists have begun developing a budding yeast (*Saccharomyces cerevisiae)* model with a fully humanized proteasome to accommodate detailed study.

To date, up to 6 of 7 alpha subunits in the 20S core of the proteasome can be humanized together, all except the α5 subunit, preventing complete humanization of alpha ring in *S. cerevisiae*. This suggests that yeast chaperones responsible for assembling the 20S proteosome complex may be incompatible with some human subunits (e.g. α5). Thus, to achieve my aim of completely humanizing the alpha ring, I created a set of genetically engineered yeast strains expressing orthologous human chaperones and investigated whether they improved proteasome humanization in yeast.

Results show that human chaperones do not complement phenotypes associated with deleting their yeast orthologs, suggesting they may be incapable of yeast proteosome assembly. Moreover, negative genetic interactions observed between human chaperones and human α5 or β2 subunits suggest these subunits may disrupt yeast 20S assembly. Human chaperone expression failed to permit humanization of α5 in strains harboring partially humanized alpha rings, suggesting that incompatible interactions involving assembly chaperones are not likely responsible for incomplete alpha ring humanization in yeast.

In conclusion, expressing human chaperones in *S. cerevisiae* failed to overcome barriers preventing complete proteasome humanization, but provided several insights to direct future studies focused on developing this model to study proteasome related diseases.

Acknowledgements

First and foremost, I would like to thank my former supervisor Dr. Aashiq H. Kachroo for giving me an opportunity to work in his laboratory, and for advising me on types of experiments I can conduct to better reinforce my hypothesis. He provided me with the freedom and support necessary to successfully complete my thesis research. I also express my gratitude to my administrative supervisor Dr. Christopher Brett who helped me write this thesis and guided me through the steps required for graduation.

I am grateful to my supervisory committee members, Drs. Elena Kuzmin and David Kwan, for their valuable feedback on my thesis research project.

I express my gratitude to Kachroo Lab members who were always supportive whenever I needed help, especially my mentor Mudabir Abdullah who assisted me almost daily in-person and has been a reassuring presence. I would also like to thank Michelle Vandeloo and Brittany Greco who helped me in Kuzmin Lab with tetrad dissections needed to complete my studies.

I am sincerely thankful to my parents who made significant sacrifices to provide me with their unwavering support throughout the duration of my M.Sc. studies.

Table of Contents

List of Figures ..... **vi**

List of Tables ..... **vii**

List of Abbreviations ..... **viii**

1. Chapter 1 – Background **1**

1.1 The proteasome and its physiological importance 1

1.2 *Saccharomyces cerevisiae* as a model to study the human proteasome 2

1.3 Genetic modularity as a strategy to drive human proteasome assembly in yeast 3

1.4 Eukaryote protein chaperones for proteasome assembly 4

2. Chapter 2 – Functional complementation suggests orthogonal interactions between human and yeast proteasome assembly chaperones **6**

3. Chapter 3 – Effect of human chaperones on partially humanized proteasome assembly **12**

4. Chapter 4 – 20S CP subunit humanization does not seem to affect proteasome localization **15**

5. Chapter 5 – Discussion **17**

5.1 Thesis summary 17

5.2 Future directions 17

6. Chapter 6 – Materials and Methods **19**

7. Chapter 7 – Bibliography **27**

List of Figures

Figure 1. Lethal genotypes from humanizing some proteasome 20S alpha subunits can be rescued by also humanizing neighboring subunits 4

Figure 2. Protein chaperones in the proteasome 20S CP assembly pathway 5

Figure 3. Genetic engineering strategy to humanize proteasome assembly chaperones in *S. cerevisiae* 8

Figure 4. Human chaperone genes do not functionally complement yeast counterparts 10

Figure 5. Human *PSMG1* and *PSMG2* do not seem to complement their yeast orthologs *PBA1* and *PBA2* 11

Figure 6. Human chaperones reduce growth of yeast strains with humanized α5 or β2 proteasome subunits 13

Figure 7. Human chaperones do not rescue defective phenotypes found in yeast with multiple humanized 20S proteasome subunits 14

Figure 8. GFP-tagged Rpn11 shows that nuclear localization is maintained in yeast with humanized proteasome alpha subunit(s) 16

Figure 9. Genetic engineering strategy to introduce GFP-tag at 3' end of RPN11 23

List of Tables

Table 1. Proteins of interest identified by mass spectrometry analysis 7

Table 2. Primers used in this study …….....23

Table 3. Yeast strains used in this study 24

Table 4. Plasmids used in this study 26

List of Abbreviations

ATP	Adenosine Triphosphate
CFU	Colony Forming Units
CP	Core Particle
CRISPR	Clustered Regularly Interspaced Short Palindromic Repeats
GFP	Green Fluorescent Protein
gRNA	Guide RNA
LB	Lysogeny Broth
MM	Magic Marker
NLS	Nuclear Localization Sequences
OD	Optical Density
PCR	Polymerase Chain Reaction
RP	Regulatory Particle
SD	Synthetic Dropout
TU	Transcription Units
WT	Wild-type
YPD	Yeast (extract) Peptone Dextrose

Chapter 1: Background

1.1 The proteasome and its physiological importance

Living cells utilize polypeptides and proteins as structural units for organismal morphology and as enzymes to facilitate nearly all biological processes. As such they make up a large proportion of the cellular biomass, e.g. more than a billion protein molecules are present in a human cell at any given time [1]. Because all protein lifetimes are finite, cells must continually biosynthesize new proteins to replace defective or unneeded proteins that undergo selective proteolysis to maintain cellular proteostasis (protein homeostasis). Defective proteins are usually formed by misfolding caused by genetic mutations or errors in transcription or translation, or by stressors, e.g. oxidation, that damage protein structure. Properly folded proteins can also be tagged for degradation when they are produced in excess or no longer needed by the cell, e.g. during tissue development when cells undergo programmed differentiation and unneeded proteins are to be cleared [2, 3]. These proteins are ubiquitylated, which allows them to be recognized by two major protein degradation processes, the endolysosomal system and the proteosome. Both catabolize polypeptides into amino acids for reuse by the biosynthesis machinery. The inability to degrade proteins leads to their aggregation and accumulation to toxic levels, which is associated with normal aging and age-related diseases such as type 2 diabetes and Alzheimer's disease [4, 5].

The proteasome is a large, multi–subunit protein complex essential for proteostasis that allows eukaryotic cell survival. It consists of the 19S regulatory particle and the 20S core particle (20S CP). Consisting of 6 Rpt (Rpt1-6) and 12 Rpn subunits, 19S RP binds both ends of 20S CP, and acts as a lid that recognizes polyubiquitin chains attached to proteins labeled for degradation. It deubiquitylates and unfolds the protein so it can be translocated to the interior of the 20S CP [6]. 20S CP is a cylinder-like complex formed by four stacked heptameric rings: two outer rings made up of α1-7 subunits (α-ring) and two inner rings composed of β1-7 subunits (β-ring) [6]. The N-termini of the alpha subunits form a closed channel that prevents access to the 20S CP interior until 19S RP binds polypeptide substrate and Rpt1-6 subunits hydrolyze ATP to open the pore [7]. The interior of the 20S CP is lined with six proteolytic sites all located within the two beta rings: each β1 has caspase-like activity, β2 has trypsin-like activity, and β5 has chymotrypsin-like activity [8, 9]. These sites ensure that proteins that enter 20S CP are digested into small peptides which are believed to exit through 19S channel at the other end of the proteasome [10].

Proteasome polymorphisms have been identified as a risk factor for multiple health conditions. *PSMA6* alone, which encodes human α1 subunit, have been linked to autoimmune diseases, metabolic diseases and cardiovascular disorders [11]. There are two general mechanisms on how malfunctioning proteasomes contribute to human disease. First, decreased proteasomal activity leads to many neurodegenerative diseases as neurons are more sensitive to damage from protein aggregates (proteotoxic stress) than other cells. For example, Parkinson's disease is hallmarked by neuronal *α*-synuclein accumulation, which can be alleviated by introduction of proteasome activator molecules that enhance 20S catalytic activity [12, 13]. Otherwise, some diseases hijack and upregulate proteasomal activity to maintain proteostasis despite increased production of damaged proteins, preventing apoptosis in diseased cells. Blood cancers like multiple myeloma, parasitic diseases like malaria, and bacterial diseases like

tuberculosis exhibit this behavior, and proteosome inhibitors have been identified as effective treatment method for these ailments [12, 14]. Study of the proteasome and its response to various stimuli therefore has significant clinical relevance.

1.2 *Saccharomyces cerevisiae* as a model to study the human proteasome

Saccharomyces cerevisiae (*Sc*; budding yeast) is a common model organism used to uncover the genetic and molecular contributors to fundamental eukaryotic cellular processes. For example, *S. cerevisiae* was used to discover (ATG) genes responsible for autophagy, a major contributor to proteostasis in all eukaryotes including humans [15]. Yeast-based studies have also proven effective in discovering enzymes and pathways responsible for ubiquitin tagging, and characterization of the transcriptional activator *RPN4* that regulates proteasome subunit expression and is critical for proteasomal activity [16, 17]. The *S. cerevisiae* genome was the first eukaryotic genome to be sequenced (in 1996), yeast genetic and protein interactions are extensively documented, and well-established protocols and tools are available for efficient manipulation of yeast genes. S. *cerevisiae* cells are easy to grow at high densities, have relatively high growth rates, are capable of efficient homologous recombination, and have haploid (or diploid) forms for relatively simple genotype-to-phenotype assessment [18, 19].

Because of its genetic amenability and high conservation of mechanisms responsible for basic cellular functions, it is frequently used for human (*Homo sapiens, Hs*) gene studies. *S. cerevisiae* and humans share thousands of orthologous genes with 43% of 414 essential genes able to be individually "humanized", i.e. replacing the yeast orthologous gene with the human one [18, 20]. Moreover, ectopic expression of human disease alleles in *S. cerevisiae* helped reveal the basis of cellular dysfunction offering insight into etiology. Introduction of human mutant genes that affect polyglutamine or α-synuclein protein allowed yeast to successfully model dysfunctions like Huntington's disease or Parkinson's disease even when no yeast homologue for the introduced gene exists, with yeast cells exhibiting cellular pathology similar to that found in mammals [21]. These yeast models of human disease are often used to identify chemicals or genetic perturbations that alleviate toxic symptoms, offering possible treatment strategies [22, 23]. Thus, we reasoned that developing a yeast model with a fully humanized proteasome will provide an effective platform for better understanding its role(s) in proteostasis and related diseases, as well as for identifying drugs that overcome toxic protein aggregation caused by malfunction of this organelle.

Towards this end, Kachroo *et al.* systematically humanized genes encoding all subunits of the proteasome in *S. cerevisiae* [20]. Most proteasome subunits in yeast and humans have one-to-one pairwise orthology. However, in cases where there are multiple human ortholog, the gene used in broader cellular context was chosen for replacement. For example, PSMA7 which encodes human α4 for non-specific proteasome was selected over PSMA8 which encodes human α4 for spermatoproteasome. It was revealed that 2 yeast subunits (Rpn3, Rpn12) in 19S RP and 5 subunits in 20S CP (β1, β2, β5, β6, β7) cannot be individually replaced by their human orthologs. However, any one of seven alpha subunits can be complemented by human subunits. Building on this result, they humanized pairs and multiples of alpha subunits and found that certain pairs (e.g. α16, α56) were not tolerated, and replacing up to 6 of 7 subunits (α123467; no

α5) in the same strain was possible **(Figure 1A)** [24]. Despite significant progress, they were unable to humanize all 7 alpha subunits and concluded that assembly of α5 into the outer ring was problematic. Thus, ***the primary aim of my thesis research is to design and test strategies to complete human 20S CP alpha ring assembly by targeting proteasome-associated proteins, such as assembly chaperones***. Anticipated outcomes will put us on path towards generating a yeast model to study the cellular (patho-) physiology of the human proteasome in more detail.

1.3 Genetic modularity as a strategy to drive human proteasome assembly in yeast

The concept of modularity posits that biological systems are organized into modules of interconnected proteins that act quasi-independently from other modules to carry out a discrete function [25]. When considering orthology, this theory suggests that genes encoding proteins within the same module are likely to exhibit similar rates of evolution [26]. If true, then yeast modules with high evolutionary rates are less likely to accommodate humanization of individual components alone, as other contributing orthologs are too divergent. Complementation of individual yeast orthologs with human counterparts does suggest that the yeast proteins belonging to the same module (i.e. pathway or complex) share similar replaceability [20]. Thus, to completely humanize the proteasome in yeast, I reasoned that a better understanding of neighboring proteins interactions within the same module is required.

The Kachroo lab previously demonstrated that humanization of proteasome subunits sometimes required strategies to address incompatible interactions between neighboring proteins within the complex. For example, humanization of the β2 subunit alone was not tolerated. This subunit has a long C-terminal tail that wraps around the neighboring β3 subunit. For compatibility, they replaced the C-terminus of human β2 with the yeast equivalent. Further investigation revealed that a serine (human)-to-glycine (yeast) substitution at position 214 (β2 S214G) was sufficient to support mutant human β2 assembly into the yeast complex. In support, β2 humanization is possible in strains expressing human β3 [27]. Together, these results suggest that irreplaceable yeast subunits can be humanized if orthogonal protein interactions are accommodated, e.g. by humanizing adjacent proteins in the same module either simultaneously or in advance. This stepwise strategy of humanizing one or more replaceable 20S CP subunits led to the construction of a viable yeast strain that has 6 out of 7 alpha subunits replaced (*Hs*-α123467). Notably, this approach overcame incompatible pairwise substitutions between α1 and α6 (*Hs*-α16), and α4 and α6 (*Hs*-α46) **(Figure 1B)**. However, the α5 subunit was not humanizable in the *Hs*-α123467 strain [24]. Pairwise humanization of alpha subunits revealed that *Hs*-α56 and *Hs*-α57 were incompatible, as were triplet and quadruplet human subunit replacements containing these pairings, e.g. *Hs*-α456, *Hs*-α457 and *Hs*-α4567. These results suggest that interactions between human α5 and its neighbors within the alpha ring are likely not responsible for observed incompatibility, and its assembly into the 20S CP is dependent on interaction with other components within this module.

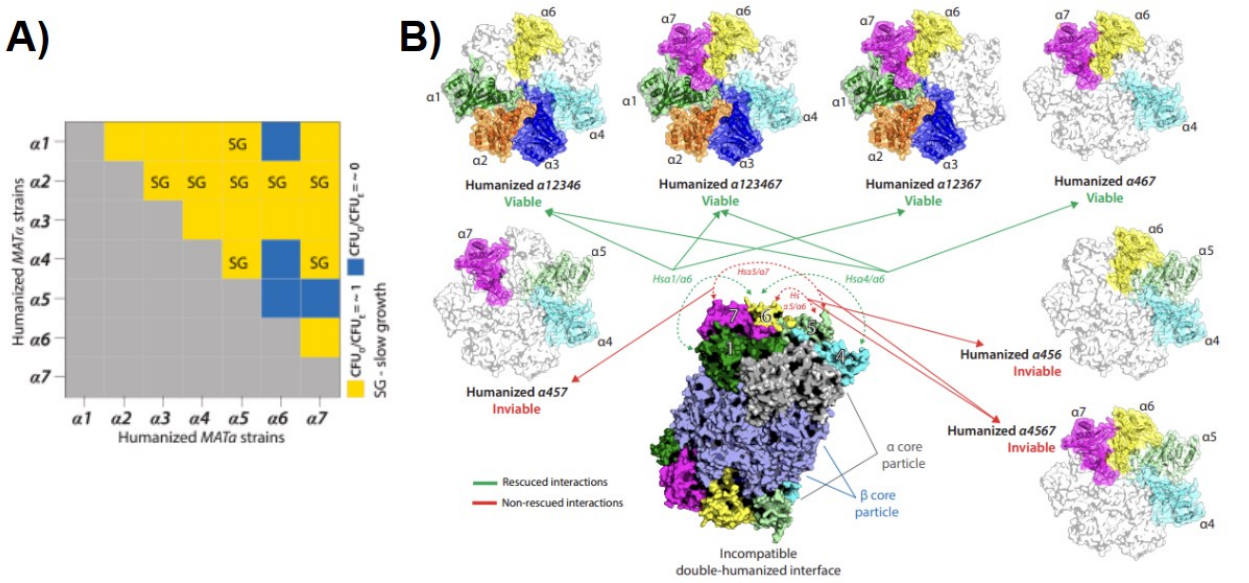

Figure 1. Lethal genotypes from humanizing some proteasome 20S alpha subunits can be rescued by also humanizing neighboring subunits. (A) Viability of yeast strains each containing a different pair of humanized alpha subunits test by haploid mating. Yellow represents viable, blue represents lethal. **(B)** Presence of additional human α subunits allows survival of strains with *Hs*-α16 and *Hs*-α14, but not strains with *Hs*-α56 or *Hs*-α57. Structures show locations of neighboring alpha subunits within the outer ring and 20S CP of the proteasome. Referenced from Abdullah *et al.* (2023).

1.4 Eukaryote protein chaperones for proteasome assembly

Pba1, Pba2, Pba3, Pba4 and Ump1 are five protein chaperones that assist with 20S proteasome assembly in yeast. Human orthologs of these chaperone proteins are PAC1, PAC2, PAC3, PAC4 and POMP encoded by *PSMG1, PSMG2, PSMG3*, *PSMG4* and *POMP* genes, respectively [28]. From what has been resolved to date, the 20S CP assembly pathway is mostly conserved suggesting that these orthologous proteins exhibit similar functions, excluding a few cases described below [29]. 20S CP assembly pathway starts with alpha ring (α-ring) formation that involve α subunits forming intermediates with each other. An intermediate containing α1, α2, and α4 forms [30] and it is thought to be recruited by α4567 intermediate formed from an unstable homo-tetradecamer of α7 subunits [31]. PAC1-PAC2 (PAC12) and PAC3-PAC4 (PAC34) heterodimers ensure that all seven α subunits are incorporated in the correct orientation by binding opposite sides of the assembling α-ring [28, 29] **(Figure 2)**. PAC34 is required for formation of an α4567 intermediate, whereas PAC12 ensures correct assembly of α567 by interacting with the α5–α6 and α6–α7 interfaces [32]. PAC34 is detached after the α-ring is fully assembled, then the β-ring starts to form using the completed α-ring as support [28, 29]. Both Ump1 and POMP help with processing β subunits, but Ump1 binds an α-ring-β234 intermediate, whereas POMP binds the α-ring first and recruits β2 to initiate β ring assembly [33]. Two completed half-mers consisting of an α-ring and a β-ring are dimerized to form a single 20S CP

that is activated by cleavage of propeptides on β subunits. Chaperones bound to the complex are then digested with the exception of Pba12 which is detached and recycled in yeast unlike human PAC12 [34].

Many reports suggest that there may be incompatibilities between yeast and human chaperones preventing assembly of human 20S CP in *S. cerevisiae*. For example, POMP is required for the human β2 subunit to bind the human α-ring whereas the yeast α-ring recruits β2 without chaperones [33]. Also, deletion of yeast Pba1 only diminishes the rate of proteasome synthesis with no noticeable cellular defects, whereas knocking out its mammalian ortholog PAC1 in mice is lethal in embryos [35, 36]. These chaperones also form extensive physical interactions with proteasome subunits. PAC12 binds all alpha subunits except α3, having a noteworthy interaction with α5, the only subunit that will not assemble into the humanized α-ring. PAC34 binds α3–α7 while also having strong interaction with α5 subunit [28, 29]. PAC34 also interacts with POMP, the chaperone that binds and stabilizes a complete α ring and mediates subsequent β ring assembly [29, 37]. Thus, I hypothesized that introduction of PAC1-4 and POMP will improve human proteasome assembly in *S. cerevisiae*, and investigated phenotype of yeast strains expressing human assembly chaperones to better understand their importance.

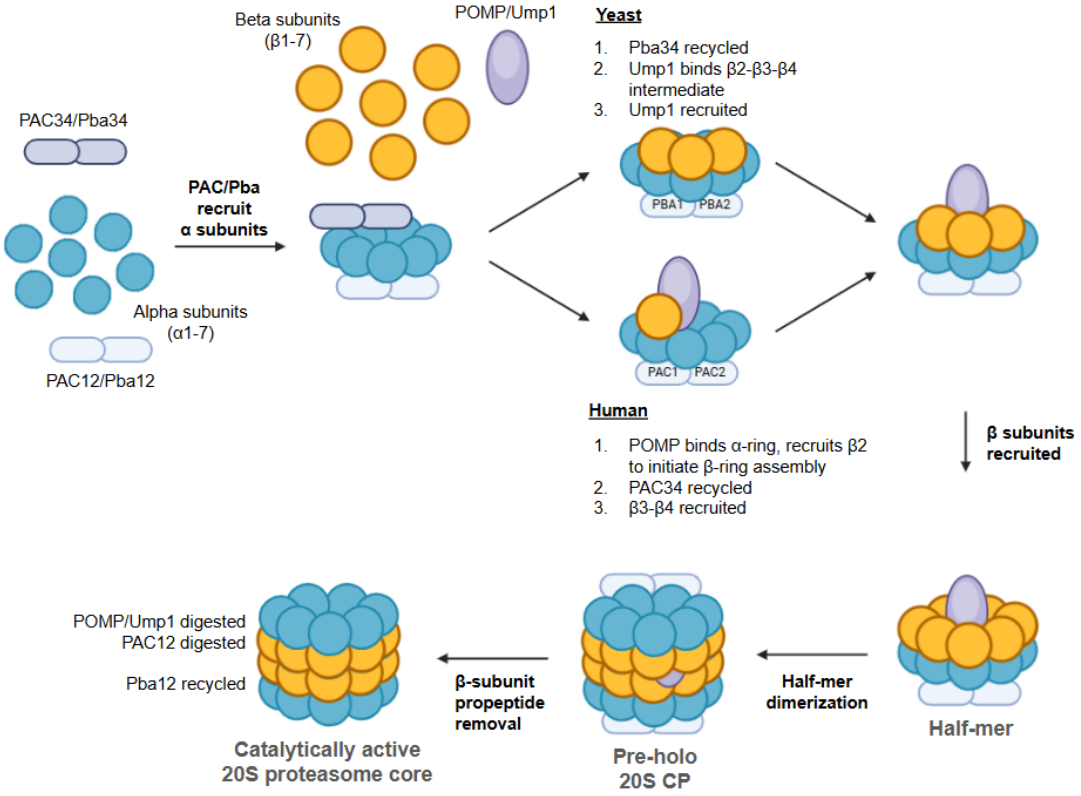

Figure 2. Protein chaperones in the proteasome 20S CP assembly pathway. PAC/Pba proteins assist with alpha subunit organization while POMP/Ump1 assist with beta subunit organization. Human POMP has an additional role of initiating beta subunit recruitment. Chaperones are named in the following manner: human/yeast.

Chapter 2: Functional complementation suggests orthogonal interactions between human and yeast proteasome assembly chaperones

To replace yeast proteasome 20S assembly chaperones with their human orthologs, I first designed a genetic engineering strategy to introduce human chaperone genes into *S. cerevisiae*: I initially generated a library of transcription units (TU) each encoding one of five human chaperone genes, a unique upstream promotor, a unique downstream terminator, and a unique set of connector sequences that flank the TU to accommodate Golden Gate-based plasmid assemblies that add them to a centromeric vector containing the *URA3* auxotrophic marker (CEN6URA; **Figure 3**). I used this set of TUs to generate a series of yeast expression plasmids that each include: only a single human chaperone (*PSMG1, PSMG2, PSMG3, PSMG4*, *POMP*), two chaperones that function as a heterodimer (*PSMG1-PSMG2* or PSMG12, *PSMG3-PSMG4* or PSMG34), four chaperones known to assist α-ring assembly (*PSMG1-PSMG2-PSMG3-PSMG4* or PSMG1234), or all five chaperones (*PSMG1-PSMG2-PSMG3-PSMG4-POMP* or PSMG1234+POMP). Golden Gate cloning products were verified by Oxford Nanopore sequencing (Plasmidsaurus).

All human chaperone genes were codon-optimized and different constitutive promoters with similar transcriptional strength were used for each chaperone gene to ensure a high and comparable level of protein expression. This also avoids overlap between promoter sequences during Golden Gate assembly that could trigger unintended homologous recombination and prevents competition for transcription factors when co-expressed. Two variants of TU4 (TU4.1 and TU 4.2) were constructed to facilitate Golden Gate assembly of multiple TU-containing plasmids that require termination of the final TU with a ConRE connector sequence **(Figure 3)**. The same principle was applied for all vectors: single TU flanked by ConLS and ConRE allowed assembly of single-gene plasmids, while TUs with ConLS-ConR1 or ConL1-ConRE connectors were used to assemble double-gene plasmids. *URA3* was selected because it enables yeast transformant survival in synthetic drop-out medium lacking uracil (SD-URA) while causing lethality in presence of 5-fluoroorotic acid, allowing both positive selection and negative selection, respectively.

To demonstrate that human chaperone proteins were expressed in yeast, I prepared whole cell lysates from wild type (BY4741) *S. cerevisiae* transformed with CEN6URA encoding all five human chaperones (CEN6URA::PSMG1234+POMP) and conducted proteomic fragment analysis by mass spectrometry. Results confirmed the presence of PAC1, PAC2, PAC3 and PAC4, as to be expected from constitutive expression. As positive controls, I found that all yeast alpha subunits were present as well as cytoskeletal proteins actin and tubulin. However, POMP protein expression could not be verified (**Table 1)**. As such, I decided to focus my experiments and discussion on PAC1-4 and their potential effect(s) on 20S alpha ring assembly. Notably, my analysis showed low amounts of the yeast proteasome assembly chaperones Pba1 and Pba2, and Pba3, Pba4, and Ump1 were not detected. Therefore, it is possible that overexpression of human proteasome assembly chaperones may downregulate expression of some yeast orthologs due to reduced demand for function in the 20S CP assembly pathway.

Table 1. Proteins of interest identified by mass spectrometry analysis

Protein FDR Confidence	Protein	Exp. Q-value	Sum PEP score	Coverage [%]	# Peptides	# PSMs	# Unique Peptides	Abundance
Transformed human proteasome assembly chaperones								
High	PAC1	0	48.644	33	10	29	10	10913874.41
High	PAC2	0	35.24	26	8	27	8	6030680.813
High	PAC3	0	50.491	58	5	20	5	10131627.34
High	PAC4	0	42.143	54	5	13	5	2279911.887
Yeast proteasome assembly chaperone orthologs								
High	PBA1	0	2.99	4	1	2	1	81945.11719
Medium	PBA2	0.047	1.392	3	1	1	1	13671.44238
Yeast proteasome alpha subunits								
High	SCL1 (α1)	0	41.499	45	11	23	11	1385531.02
High	PRE8 (α2)	0	27.531	28	5	8	5	518908.1797
High	PRE9 (α3)	0	35.217	27	7	12	7	460799.3984
High	PRE6 (α4)	0	20.691	17	3	6	3	624258.4063
High	PUP2 (α5)	0	34.201	33	9	18	9	1034335.387
High	PRE5 (α6)	0	42.255	49	8	14	8	2478362.078
High	PRE10 (α7)	0	21.77	19	4	7	4	658340.5938
Yeast cytoskeletal proteins (control)								
High	ACT1	0	166.292	67	19	74	19	21624750.98
High	TUB1	0	32.987	22	8	12	8	947859.2266
High	TUB2	0	42.28	30	8	9	8	1150284.703

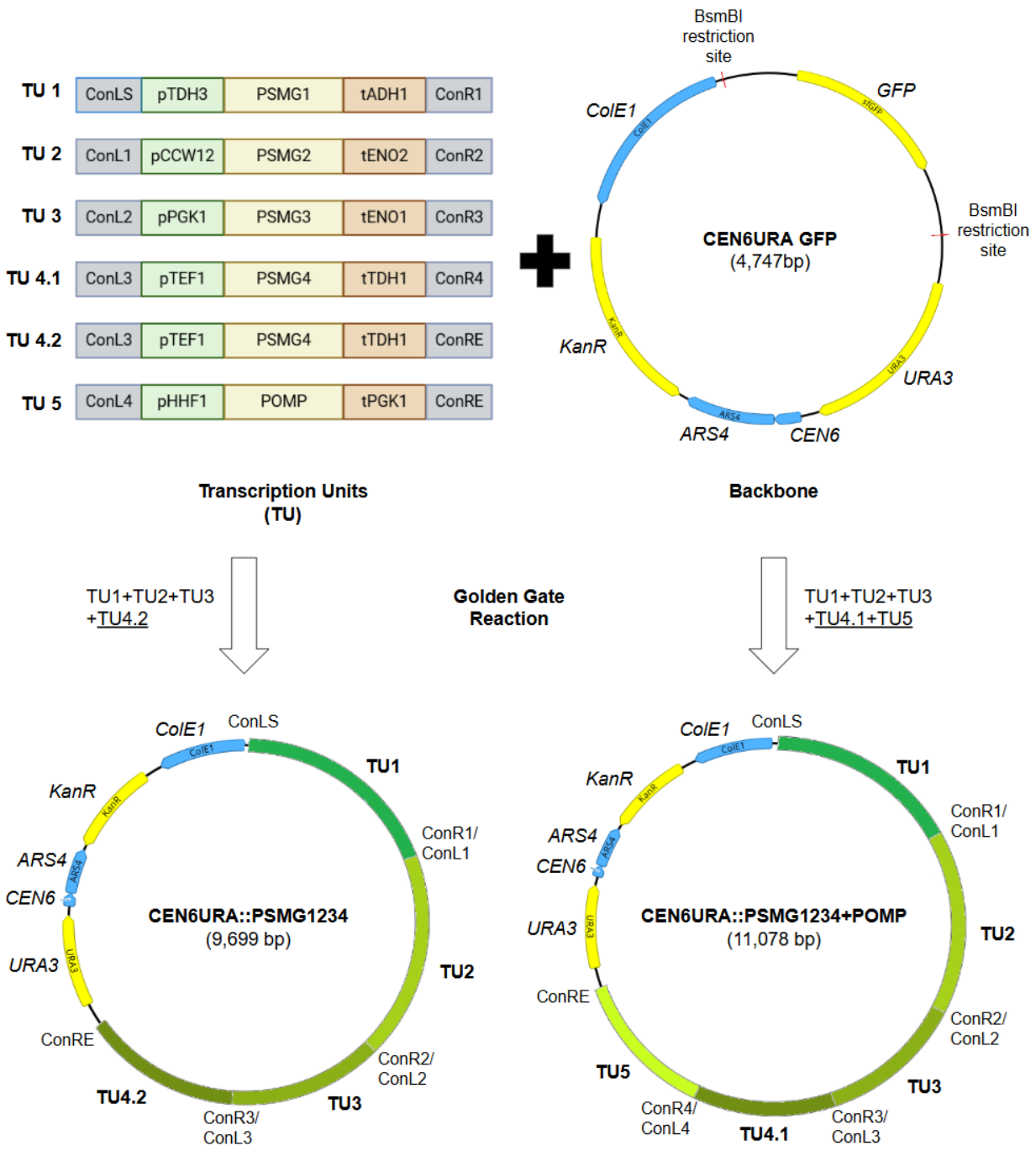

Figure 3. Genetic engineering strategy to humanize proteasome assembly chaperones in *S. cerevisiae*. Description of transcription unit (TU) library used to construct all plasmids for human chaperone expression in yeast, including CEN6URA::PSMG1234 and CEN6URA::PSMG1234+POMP which required different variants of TU4. Plasmid maps show verified assemblies of these circular plasmids, including locations of the origin of replication (CEN), yeast auxotrophic marker (URA3) and multiple TUs. ConLS and ConRE have BsmBI recognition sites that allow for incorporation into centromeric backbone.

Next, I humanized yeast proteasome chaperones of interest by transforming plasmids containing human chaperone genes into *S. cerevisiae* missing genomic copies of their yeast orthologs. To account for the possibility that the presence of individual yeast chaperone genes may be essential, I transformed diploid yeast from the Magic Marker strain collection to generate humanized strains, ensuring that all are created using the same genetic strategy for proper comparison. Each Magic Marker diploid strain is a heterozygous knockout, whereby one chromosomal copy of a yeast chaperone gene is wild-type (for survival) and the other is disrupted by the selection marker gene KanMX and a *MFA1pr-HIS3* reporter [38]. After sporulation, only MAT-a haploid cells harboring the knockout will survive on Magic Marker growth medium if viable (M.M. + G418; see Chapter 6: Materials and Methods). Thus, sporulated transformants grown on M.M.+ G418 represent humanized haploid yeast expressing the human chaperone gene of interest in place of their yeast ortholog.

I predict that deletion of yeast chaperone genes will prevent efficient assembly of the 20S CP complex. In turn, limited proteasome function should alter proteostasis, reducing protein turnover and permitting accumulation of toxic misfolded proteins, that should result in a growth defect. Replacing the yeast gene with the human gene should rescue any observed growth phenotype if they are functionally compatible. I tested functional complementation by conducting a standard colony forming unit (CFU) outgrowth assay under standard growth temperatures (30˚C; **Figure 4**). First, I found that all single null mutants are viable, consistent with previous reports [39]. When comparing knockout strains, I found that *pba3*Δ and *pba4*Δ seemed to grow more slowly than other deletion strains. Humanizing each chaperone gene showed varying effects: Replacing yeast *PBA1* or *PBA4* with human *PSMG1* or *PSMG4,* respectively, seemed to cause further, mild growth defects. Replacing yeast *PBA2* or *PBA3* with human *PAC2* or *PAC3* showed no effect on growth. Because human PAC3 and PAC4 form a heterodimer to function, I also tested if expressing both in *pba3*Δ or *pba4*Δ cells affected growth. Results show no notable effect compared to single subunit replacement, suggesting that adding the partnering human subunit does not influence dimer function in yeast.

Because I did not observe any complementation under standard growth conditions, I repeated the CFU assays at 37˚C to induce mild proteotoxic stress. The higher temperature enhances the probability of protein misfolding and thus yeast survival and growth is more dependent on proteasome function to clear damaged, toxic proteins [40, 41]. High temperature had relatively little effect on *pba1*Δ or *pba2*Δ growth, whereas *pba3*Δ and *pba4*Δ failed to grow, consistent with observed growth phenotypes at 30˚C **(Figure 4).** No changes in growth were observed at 37˚C when human chaperones were added to any of these mutants. From these initial results, I speculate that PBA3 and PBA4 may be more important than PBA1 and PBA2 for efficient yeast proteasome assembly. They also suggest that human chaperone genes cannot functionally complement their yeast orthologs when replaced individually.

Because knocking out *PBA1* or *PBA2* alone seems to have little effect on growth, I reasoned that deleting both in the same strain may show a more prominent phenotype as they are thought to optimally function as a heterodimer. To construct the *pba1*Δ*pba2*Δ double knockout strain, I mated a haploid strain (dma3254) that has *PBA1* replaced by the G418 resistance gene, with a compatible haploid strain (SN3476) that has *PBA2* replaced by the NAT resistance gene. I then sporulated the resulting diploid and dissected the tetrad to isolate haploid spores that grew on both G418 and NAT (indicating double knockout genotype; **Figure 5A)**.

*pba1*Δ*pba2*Δ haploid spores did not show any visible growth defect when compared to wild type and *pba1*Δ spores grown under standard conditions (30˚C on YPD for 48 hours). To possibly reveal a difference in growth rate, I conducted a CFU assay and reduced temperature to 25˚C in an attempt to slow down outgrowth. Under these conditions, the *pba1*Δ*pba2*Δ strain showed a small growth deficiency, suggesting that both double and single deletions of these chaperone genes may have little effect on proteasome assembly needed for function under these conditions **(Figure 5B)**. Moreover, adding their human orthologs together or individually to wild type or *pba1*Δ*pba2*Δ yeast had no effect on growth. Although further studies are necessary, these initial results suggest that human chaperones cannot functionally complement their yeast counterparts, indicating that yeast and human assembly chaperones likely have orthogonal interactions.

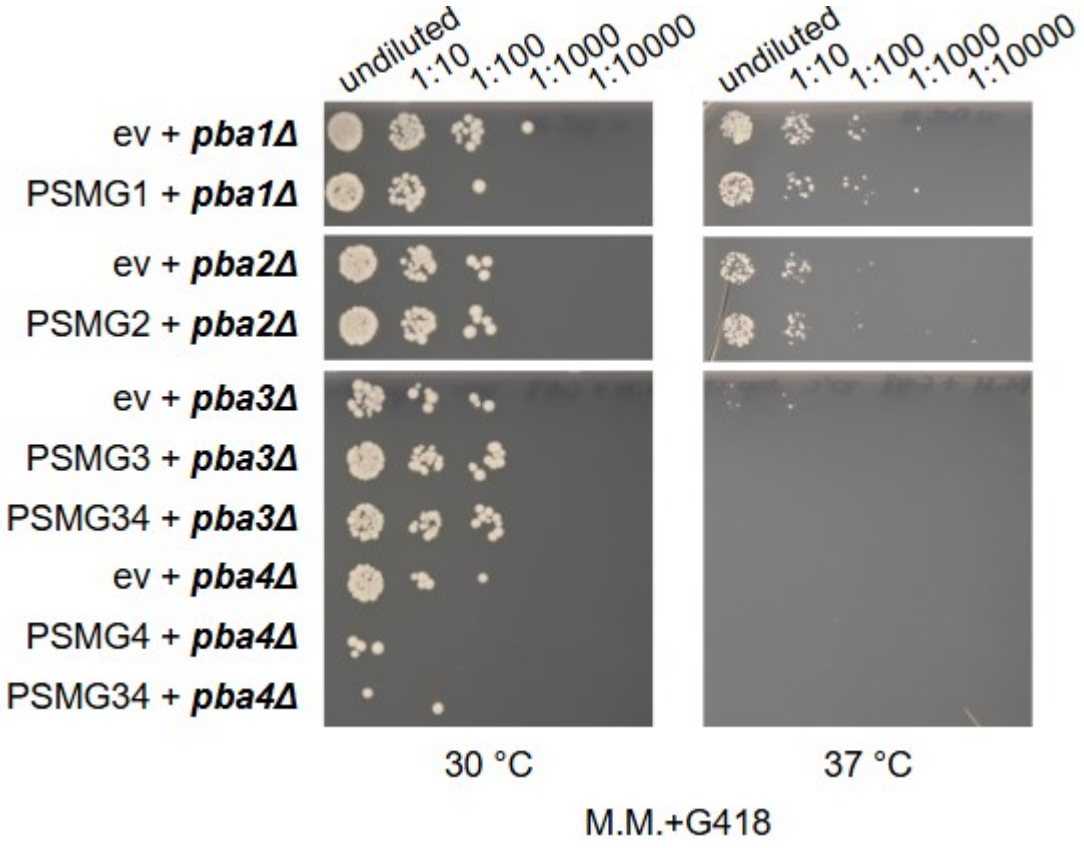

Figure 4. Human chaperone genes do not functionally complement yeast counterparts. *pba1*Δ, *pba2*Δ, *pba3*Δ, or *pba4*Δ were transformed with an empty vector (ev; CEN6URA::GFP) or an expression vector containing their human ortholog, or in some cases, two human chaperone genes. Yeast cultures were plated on magic marker (M.M) + G418 solid medium at dilutions shown and then grown at 30˚C or 37˚C for 3 days prior to being imaged.

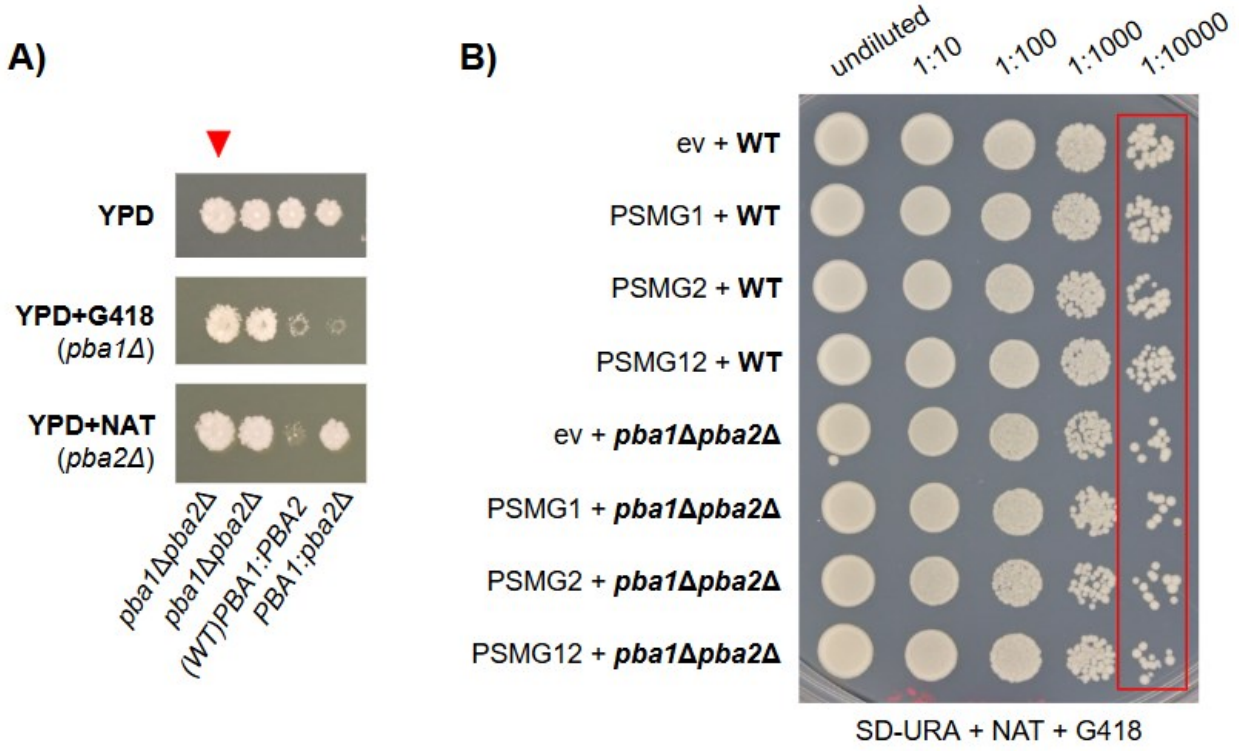

Figure 5. Human *PSMG1* and *PSMG2* do not seem to complement their yeast orthologs *PBA1* and *PBA2*. (A) Tetrad dissected from a dma3254 (*pba1*Δ::G418) x SN3476 (*pba2*Δ::NAT) diploid were outgrown on YPD or selective medium (30°C for 2 days) to assess phenotype and genotype, respectively. Red arrowhead indicates the double-null haploid mutant selected for transformation with human chaperone genes. **(B)** Wild type (WT; BY4741) or *pba1*Δ*pba2*Δ were transformed with an empty vector (CEN6URA) or one containing human PSMG1, PSMG2 or both. Serial dilutions of cultures were spotted on selective medium, and yeast were outgrown at 25˚C for 2 days prior to being imaged. Red box indicates dilution used to assess possible growth phenotypes.

Chapter 3: Effect of human chaperones on partially humanized proteasome assembly

Because adding up to two human chaperones to yeast showed little effects, I next determined if adding all four PSMG may show a phenotype. Moreover, my preliminary results suggest that human chaperones may not interact with yeast proteasome subunits. Thus, I also tested whether humanizing individual alpha subunits could drive a potential interaction that would be observed as a change in growth rate if proteasome assembly was affected. To do so, I transformed either an empty vector (CEN6URA; control) or one encoding 4 human chaperone genes (CEN6URA::PSMG1234) into yeast strains which had a single 20S CP subunit substituted with its human ortholog: *Hs*-α1, *Hs*-α2, *Hs*-α3, *Hs*-α4, *Hs*-α5, *Hs*-α6, *Hs*-α7, *Hs*-β3 or *Hs*-β4. To check compatibility with the human β2 subunit, I introduced the vectors into strains containing *Hs*-β2β3 or a *Hs*-β2 S214G mutant which are required for human β2 integration into the yeast proteasome [27]. I then measured the growth of SD-URA liquid culture over time by monitoring the optical density at 595 nm (O.D. 595 nm) at 30˚C over three days of incubation. Upon comparing their growth rates by calculating doubling time, I found that introducing these human chaperones into wild type or humanized yeast strains had no discernable effect on growth, apart from yeast containing either human α5, β2β3 or β2 S214G which all exhibited slower growth rates (**Figure 6A**). Incompatibility resulting from an interaction between human chaperones and *Hs*-α5 is particularly intriguing because it may be relevant to the previously reported *Hs*-α56 lethal genotype that prevents humanization of the complete alpha ring (see **Figure 1**; [24]).

To further investigate these potential genetic interactions, I sought to identify the specific chaperone(s) that may be responsible for observed growth defects. *Hs*-α5 or *Hs*-β2β3 strains were transformed with vectors containing single chaperones (*PSMG1*, *PSMG2*, *PSMG3*, *PSMG4*) or two heterodimeric chaperones (*PSMG12*, *PSMG34*) and these were compared to one containing all 4 PSMG chaperones (*PSMG1234*) or none. I found that transformants with single human chaperones or heterodimers all had similar growth phenotypes as strains without human chaperones (**Figure 6B**). Thus, all four human PAC chaperones need to be present to induce negative growth. The possibility that growth inhibition occurred due to toxicity from overexpression of transformed DNA is low since most strains that express all four chaperones from a large plasmid do not exhibit growth defects (**Figure 6A**).

From these results, I speculate that introduction of human assembly chaperone results in dominant negative effect. Reduced growth may be due to incompatibility caused by protein-protein interaction between human α5, β2 subunit and the proteasome assembly intermediate involving all four PAC chaperones (**Figure 6C**). For example, binding of human PAC12 and PAC34 heterodimers to a fully or partially assembled alpha ring could induce conformational changes that make it incompatible with *Hs*-α5 or *Hs*-β2 that must still be recruited, preventing assembly of a complete proteasome.

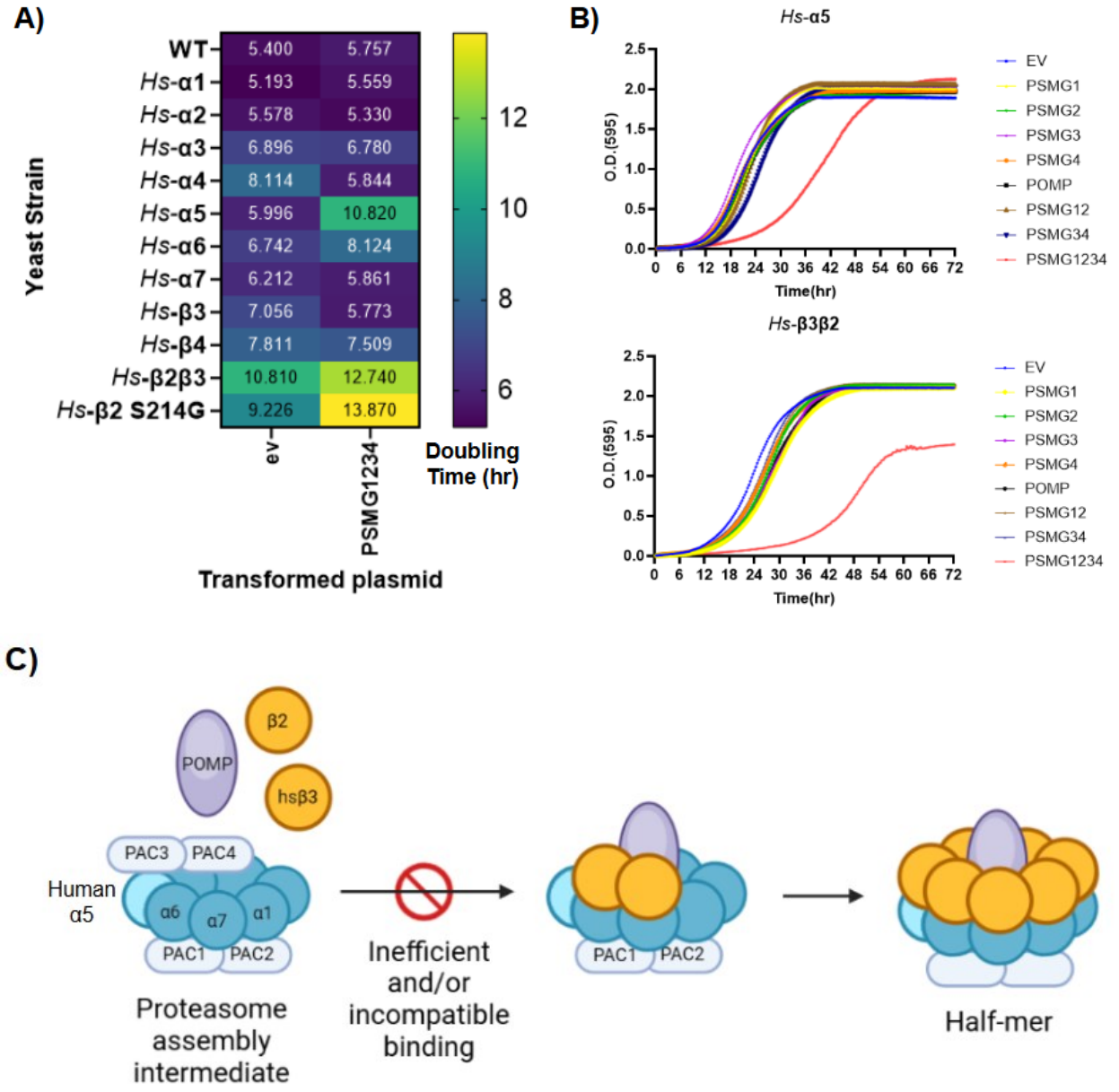

Figure 6. Human chaperones reduce growth of yeast strains with humanized α5 or β2 proteasome subunits. (A) Heatmap for doubling time of WT and partially humanized yeast strains expressing four human PAC chaperones or none. Doubling time was obtained from logarithmically transformed O.D. 595 nm values for enhancing contrast (see Chapter 6: Materials and Methods). **(B)** 72-hour growth curve of *Hs*-α5 or *Hs*-β2β3 strains transformed with single, double, or all four human PSMG genes. The red line represents yeast expressing PSMG1234 human chaperones, which was the only transformant to grow slower than WT. **(C)** Graphical representation of proposed model where binding of human PSMG heterodimers to yeast 20S subunits or human α5, β2 subunit create assembly intermediate that cannot recruit the other, preventing half-mer proteasome formation.

Since the presence of all four PSMG chaperones have been demonstrated to affect transformant phenotypes, I investigated whether they can rescue the defects resulting from multiple humanized 20S CP subunits. *Hs*-α6 and *Hs*-α12347 are sensitive to high temperature, meaning integration of human subunit(s) into proteasome can diminish proteasome function [24]. All alpha subunits interact with either one or both of PSMG heterodimers, so I have transformed CEN6URA::PSMG1234 into not only *Hs*-α12347, but also *Hs*-α123467 and *Hs*-α12347β3 which have additional humanized subunits to increase the probability of rescue. Unfortunately, PAC1-4 expression did not allow these partially humanized strains to grow in 37°C **(Fig 7A)**.

Since both PAC12 and PAC34 have been reported to interact with α5, and negative interaction between human α5 and PAC1-4 complex has been identified, I next examined whether the presence of all human chaperones can rescue *Hs*-α56 lethal genotype. Experiment was carried out with yeast strain with humanized α4, α6, α7 that expresses both yeast and human α5 (*Hs*-α467homo5het), as it can easily be converted into lethal *Hs*-α4567 genotype by CRISPR knockout of *PUP2* that encodes yeast α5. *Hs*-α467homo5het was first transformed with CEN6G418::PSMG1234+POMP. I have constructed a new plasmid with G418 selection since CRISPR guide RNA, that binds *PUP2* coding region and permanently inactivates it by inducing double-stranded break, used *URA3* selection marker. Subsequent transformation of two *PUP2*-specific CRISPR guide RNAs into *Hs*-α467homo5het has resulted in no survivors even when human chaperones were present **(Fig 7B)**. Absence of human assembly chaperones are therefore not the primary factor responsible for lethality observed in *Hs*-α56.

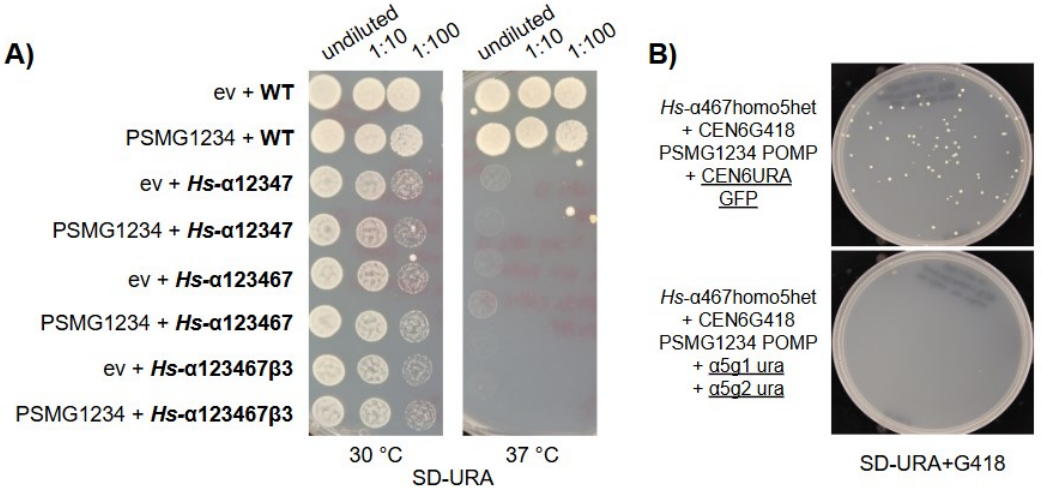

Figure 7. Human chaperones do not rescue defective phenotypes found in yeast with multiple humanized 20S proteasome subunits. (A) WT and temperature-sensitive strains that have humanized α12347 subunits were transformed with an empty vector or four human PSMG chaperone genes. Colonies were plated on synthetic dropout media without uracil (SD-URA) and then grown at 30˚C or 37˚C for 3 days. **(B)** *Hs*-α467homo5het with all human chaperone genes were grown at 30˚C for 7 days. Control colonies transformed with empty vector survived, while colonies transformed with guide RNA did not survive conversion to *Hs*-α4567 genotype.

Chapter 4: 20S CP subunit humanization does not seem to affect proteasome localization

Proteasomes have been found to be predominantly localized in the nucleus of non-quiescent, unstressed yeast cells. Localization of the mammalian proteasome is less conclusive, but mammalian nuclei also maintain high levels of proteasome [42, 43]. There are multiple studies which strongly suggest that this nuclear localization is required for maintenance of proteostasis in the nucleus [44-47]. AKIRIN2 binds directly to α3/α4 subunits of 20S CP in humans and is essential for nuclear import of the proteasome; depletion of AKIRIN2 in vertebrate cells have resulted in daughter cells that do not have proteasomes within their newly formed nuclei, with high enrichment of transcription factor MYC and other nuclear proteins indicating that regulation of these protein levels require nuclear proteasome localization [44]. Moreover, cytosolic proteins can also be imported into the nucleus for proteasomal degradation [45, 46]. When misfolded proteins are aggregated into temporary compartments due to the ubiquitin-proteasome system being overloaded by high production of defective proteins, cytosolic misfolded proteins have been observed to be evenly distributed to compartments outside and within the nucleus [47], demonstrating that a significant amount of proteasomal degradation occurs inside the nucleus.

20S CP assembly that initiates the construction of a proteasome occurs in the cytoplasm [48]. Proteasomes must therefore be actively transported into the nucleus to maintain their nuclear localization as demonstrated by an AKIRIN2 depletion study from Almeida *et al.* (2021). Nuclear localization sequences (NLS) that allow binding of importins, proteins that transfer bound cargo into the nucleus, have been identified in yeast subunits α1, α4, α5 and human subunits α1-4 [43]. Although three proteasomal NLS are conserved from yeast to humans, CP precursor complexes are transported into the nucleus then assembled into a proteasome for yeast, while only fully matured proteasomes are transported into the nucleus for humans [43, 44]. Human PAC12 heterodimer binding is believed to prevent CP assembly intermediate from being imported [32]. It was therefore hypothesized that disrupted proteasome localization may be responsible for aberrant or lethal phenotypes triggered by humanization of 20S CP subunits, since nuclear proteasome import requires protein-to-protein interaction with 20S CP, with yeast and human having different timing on when the proteasome or its assembly intermediates are transferred.

I have used homologous recombination to integrate GFP with *HIS3* auxotrophic marker (GFP-tag) at the 3' end of *RPN11* in *Hs*-α1, *Hs*-α2, *Hs*-α3, *Hs*-α4, *Hs*-α5, *Hs*-α6, *Hs*-α7 and *Hs*-α123 strains (see Chapter 6: Materials and Methods; **Figure 9**). *RPN11* is a component of 19S RP identified to be a reliable tracker of the proteasome lid [43]. Although most 20S CP subunits can be tagged without issue, introducing a GFP tag to the β5 subunit have been reported to induce aberrant proteasome localization in WT yeast [49]. Direct tagging of α or β proteasome subunits was therefore avoided since impact of their humanization on the 20S CP structure is unclear, and it was difficult to predict potential disruptive effects that may occur from GFP-tag attachment. Rpn11-tagging of *Hs*-α123467β3 was also attempted but resulted in no survivors,

which may suggest that the proteasome within the strain has low structural integrity and cannot tolerate Rpn11 modification.

Fluorescent microscopy of tagged transformants grown up to optical density of 1.5 at 595 nm revealed that GFP signal was consistently localized within the nucleus, including *Hs*-α6 which was heat intolerant (**Fig 8**). This preliminary result suggests that replacement of a yeast 20S subunit with human orthologs does not seem to affect nucleocytoplasmic transport of the proteasome.

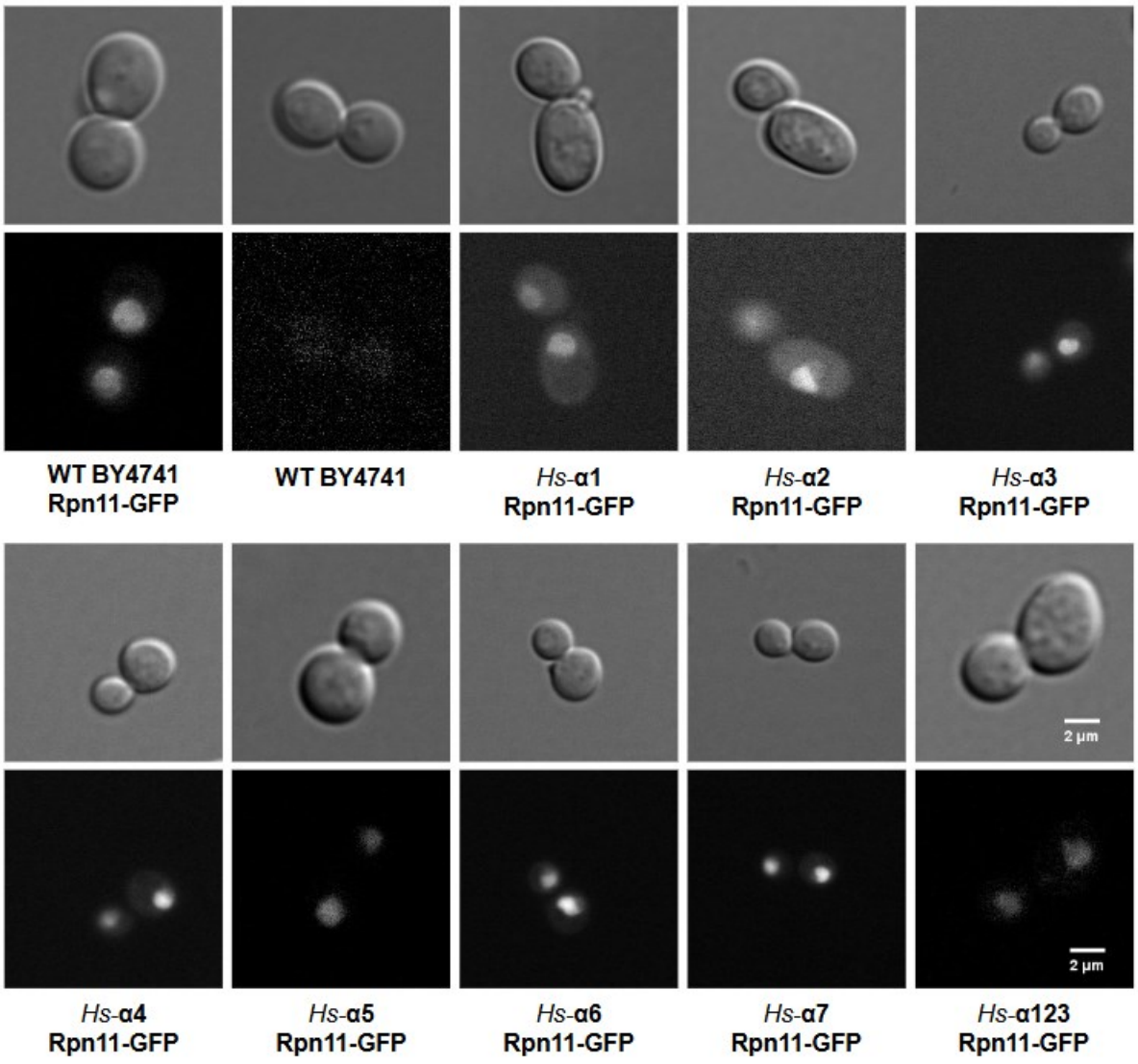

Figure 8. GFP-tagged Rpn11 shows that nuclear localization is maintained in yeast with humanized proteasome alpha subunit(s). Negative control (WT BY4741) and strains expressing Rpn11- GFP were observed under brightfield (above row) and GFP (below row) setting. Lower limits of display range were set to 224 for brightfield images and 107 for GFP images.

Chapter 5: Discussion

5.1 Summary

In this thesis, I transformed human *PSMG1-4* and *POMP* into *S. cerevisiae* and investigated their effects on cell fitness to assess whether they contribute to assembly of the 20S proteasome. Functional complementation tests revealed that human chaperones cannot substitute for their yeast orthologs, suggesting that assembly chaperones may only interact with subunits from their own species. Negative genetic interactions between the human PAC1-4 complex and human α5, human β2 indicate that orthogonal chaperone activities may disrupt yeast proteasome assembly. Although it seems counterintuitive that human chaperone expression leads to decreased growth in some strains expressing human 20S subunits, I speculate that this observation relates to the concept of genetic modularity and fitness effects of humanization: Introduction of human chaperones into the predominantly yeast 20S CP assembly pathway (defined as a module) may decrease compatibility between its members (i.e. subunits). The cooperative model of high order humanization suggests that relative fitness of strains expressing PAC-4, human α5, and/or human β2 should be restored when other members of 20S CP pathway are humanized [50]. A similar pattern was observed when humanizing the sterol biosynthesis pathway in *S. cerevisiae* whereby replacing each yeast gene reduced growth until more than seven members of the pathway were humanized, whereafter growth recovered [51]. These findings therefore suggest the possibility that *PSMG1-4* are module components that directly influence replaceability of 20S proteasome subunits.

Growth sensitivity to heat stress in *Hs*-α12347, *Hs*-α123467, *Hs*-α123467β3 and lethality in *Hs*-α56 were not rescued by introduction of human chaperones suggesting that these defects are a result of human alpha subunits being incompatible with unknown yeast protein(s). Analysis of 19S RP localization with Rpn11-GFP shows that individual humanization of alpha subunits that interact with importins do not affect proteasome localization. Therefore, human alpha subunits do not disrupt proteasomal activity by being incompatible with nuclear import pathways important for proteostasis and cell survival.

5.2 Future Directions

I envision multiple experiments that should be conducted in the future to reinforce and build on my key findings: For complete functional complementation assessment of *PBA1* and *PBA2* (see Chapter 2), I recommend subjecting *pba1*Δ*pba2*Δ strains to conditions that promote proteotoxic stress that will increase dependence on the proteasome for growth and survival. For example, heat stress seems ideal because proteasome alpha subunits which PBA12 help assemble are linked to thermotolerance in yeast [41].

Nuclear localization experiments described in Chapter 4 tested the impact of humanizing only a single human proteasome subunit. Potential disruption by humanizing multiple 20S subunits should be tested to determine if this contributes to observed incompatibility. Moreover, since subunits can be imported independently in yeast unlike in humans, 19S RP localization may not necessarily represent complete 20S CP assemblies or intermediates. To address this, I I recommend the same approach but with tagging GFP to each alpha subunit of *Hs*-α123467β3 to

definitively show humanized 20S CP nuclear localization and to potentially reveal association between nuclear import and negative growth phenotypes that result from humanization of multiple alpha subunits.

My thesis research only examined heterozygous yeast strains that express both human and yeast chaperones. Having both orthologs present may interfere with human chaperone activity. Thus, I recommend complete replacement of yeast with human chaperone genes and predict that this may permit full humanization of the alpha ring. Although the effects of knocking out all yeast chaperones are unknown, I found that the relative fitness of yeast chaperone single and double null mutants were similar to wild type yeast under normal growth conditions. Thus, it may be possible that a *pba1*Δ*pba2*Δ*pba3*Δ*pba4*Δ*ump1*Δ quintuple knockout is viable but I predict that it would be very sensitive to proteotoxic stress, a characteristic that may be used to better assess humanization of 20S subunits, especially α5 and β2 which are incompatible in the presence of yeast assembly chaperones. This would eliminate potential negative interactions between yeast chaperones and human subunits that may prevent proper alpha ring assembly with or without human chaperones present.

To completely humanize the alpha ring, I recommend conducting genetic variant analysis to identify mutants that may accommodate interactions that overcome *Hs*-α56 lethality in yeast. This would involve generating a library of *Hs*-α5 mutants by random mutagenesis and then transforming it into a *Hs*-α467homo5het strain prior to yeast α5 knockout to isolate mutants that permit survival. Viable *Hs*-α5 mutants will then be sequenced revealing the subunit interface(s) required for complete humanization of yeast 20S CP.

Studying humanized proteasomes in yeast can act as a foundation to test effectiveness of potential therapies in a unicellular context before moving onto more extensive animal studies. Although my research did not identify orthogonal interactions preventing full α-ring humanization, it suggests that yeast Pba1-4 chaperones are likely unable to correctly assemble the human 20S proteasome. I therefore propose that *PBA* genes as well as all proteasome subunit genes be humanized in *S. cerevisiae* for this model to best reflect human proteasome biology.

Chapter 6: Materials and Methods

Growth media

All reagents used to prepare sterilized yeast (YPD, SD, SD-URA, SD-HIS) and bacterial (LB) growth media were obtained from Sigma-Aldrich unless otherwise specified. Synthetic complete (SC) medium was prepared with BD Difco™ Yeast Nitrogen Base without Amino Acids (Fisher Scientific), bacteriological agar, and dextrose. Magic Marker medium was made with yeast nitrogen base without amino acids and ammonium sulfate, glutamate, SC-Arg-His-Leu-Ura (Sunrise Science Products) mix, bacteriological agar, and dextrose. Sporulation medium was made with sporulation amino acid supplement, potassium acetate, yeast extract (Gibco), and bacteriological agar. Antibiotics used in this study were carbenicillin, G418 (Gibco), and nourseothricin (Werner Bioagents).

Construction of yeast expression vectors

Oligonucleotides for plasmid construction were obtained from Integrated DNA Technologies. Parts from the Yeast ToolKit [52] were assembled using BsaI-mediated Golden Gate reactions to create entry vectors (pYTK095; AmpR-ColE1) containing transcription units. These were integrated into CEN6URA expression plasmids using BsmBI-mediated Golden Gate reactions. Reactions (10 µl) contained 20 fmol DNA, 1µl FD Buffer (NEB), 1µl ATP (Thermo Scientific), 1µl T7 ligase (NEB), 1µl restriction enzyme (ThermoFisher) and water. Resulting plasmids were amplified by transforming the reaction into competent *E. coli* (NEB). Single non-fluorescent colonies were picked and inoculated overnight in 5 ml LB broth with appropriate selection, and amplified plasmids were purified from the culture using a QIAprep Spin Miniprep Kit (Qiagen, Cat.# 27106).

Yeast transformation

Yeast transformations were conducted using the Frozen-EZ Yeast Transformation II™ Kit from Zymo Research (T2001). Competent cells (comp cells) were made by adding 1 ml of Frozen-EZ Yeast Solution 1 to cell pellet from 5 ml overnight yeast culture centrifuged at 3500 rpm for 5 minutes. After another centrifugation followed by the removal of the supernatant, comp cell pellet was resuspended on 20 - 120 µl of Frozen-EZ Yeast Solution 2 depending on pellet size. The resultant solution was divided into fresh Eppendorf tubes, each containing 20 µl, for either -80°C storage or immediate transformation. For transformation, 500 µl of Frozen-EZ Yeast Solution 3 along with up to 500 ng of DNA to be transformed was added to yeast comp cells, then incubated at 30°C for 45 minutes with vortexing each 15 minutes. If the selection method was antibiotic resistance, this was followed up by 1.5-hour recovery in YPD broth, so the transformed cells were given time to express. Glass beads were used to spread ~150 µl of transformation mixture on an agar plate with appropriate selection, which was then incubated at 30°C for 2 ~ 7 days depending on the growth rate of the transformant. Presence of transformed gene was verified through colony PCR.

Protein extraction and anaylysis by mass spectrometry

Proteins from yeast transformants expressing human chaperones were extracted using a published protocol developed in the Koshland lab: 5 ml of yeast culture grown to O.D. 1.0 was collected and centrifuged for 3 minutes at 3,000 rpm (Eppendorf 5430R Centrifuge) to collect yeast cells. The pellet was then resuspended in 1.5 ml 50 mM Tris, PH 7.5 and transferred to a 1.5 ml microcentrifuge tube containing 0.2 g of 0.5 mm glass beads and 50 µl of 2% SDS and EDTA-free Protease Inhibitor Cocktail (Roche #11836170001). Yeast cells were then lysed by repeating the following cycle 3 times: vortex samples for 20 seconds then place them on ice for 1 minute. Samples were incubated at 95°C for 3 minutes, 75 µl of 3X Laemmli sample buffer (FisherScientific #J61337) was added, and the samples were incubated again at 95°C for 1 minute. Samples were centrifuged at 13,000 rpm for 10 minutes, and supernatants were collected for immediate analysis by SDS-PAGE and the remainder was stored at -20°C.

Samples were loaded into ExpressPlus™ polyacrylamide gels next to lanes containing different amounts of BSA as standards. SDS-PAGE was stopped when the dye from Laemmli Buffer reached the boundary between resolving gel and stacking gel in order to excise the entire proteome from a small area. After 1 hour of Coomassie Blue staining, the gel was destained overnight in 50ml AcOH and 50ml MeOH in 400ml dH_2O. Density of BSA and protein sample bands were compared to estimate sample protein concentration, and sample bands were excised and transferred to 1.5ml microcentrifuge tubes.

In-gel trypsin digestion was then conducted using a protocol provided by the Centre for Biological Applications of Mass Spectrometry CBAMS) at Concordia University: Gel samples were first reduced for 30 minutes at room temperature in 50mM NH_4CO_3 (Sigma) containing 10mM DL-Dithiothreitol (Sigma), then alkylated in darkness for 30 minutes at room temperature in 50mM NH_4CO_3 containing 50mM iodoacetamide (Sigma). Gel pieces were then incubated at room temperature for 15 minutes in 50mM NH_4HCO_3, followed by 15 minutes in 25mM NH_4HCO_3 with 5% acetonitrile (ACN), 30 minutes in 25mM NH_4HCO_3 with 50% ACN. Gel pieces were then incubated for 30 minutes in 25mM NH_4HCO_3 with 50% ACN again, and then for 10 minutes in 100% ACN. A speed vac at 43°C was then used to completely dry the gel piece within the microcentrifuge tube. Dried gel pieces were incubated overnight at 37°C with 50µl 25mM NH_4CO_3 containing 0.01µg/µl trypsin (Sigma). After removing the digest solution, the gel was incubated for 15 minutes at room temperature in 200µl extraction solution of 60% ACN with 0.5% formic acid (Fisher). The solutions were collected in a fresh 1.5ml microcentrifuge tube, and the extraction was repeated twice more before drying the samples with a speed vac at 43°C prior to storage at -20°C.

Samples were analyzed by liquid chromatography-tandem mass spectrometry (LC-MS/MS) in CBAMS using a Thermo EASY nLC II LC system coupled to a Thermo LTQ Orbitrap Velos mass spectrometer equipped with a nanospray ion source. Tryptic peptides were resuspended in a solubilization solution containing 97% water, 2% acetonitrile (ACN) and 1% of formic acid (FA) to give a peptide concentration of 40 ng/µL. A volume of 5 µL of each sample was injected onto a 10 cm × 100 µm column in-house packed with Michrom Magic C18 stationary phase beads (5 µm diameter, 300 Å pore size). Peptides were eluted using a 120min gradient at a flow rate of 400 nL/min with mobile phase A (96.9% water, 3% ACN and 0.1% FA) and B (97% ACN, 2.9% water and 0.1% FA). The gradient started at 2% B, linear gradients

were achieved to 8% B at 14 min, to 12% B at 41 min, to 24% B at 100 min, to 32% B at 108 min, to 87% B at 111 min, then followed by isocratic with 87% B for 3 min and with 2% B for 6 min. A full MS spectrum (m/z 400-1400) was acquired in the Orbitrap at a resolution of 60,000, then the ten most abundant multiple charged ions were selected for MS/MS detection in a linear trap with the option of dynamic exclusion. Peptide fragmentation was performed using a collision induced dissociation at normalized collision energy of 35% with activation time of 10 ms. The spectra were internally calibrated using polycyclodimethylsiloxane (m/z 445.1200 Da) as a lock mass.

Mass spectrometry data was processed using Thermo Proteome Discoverer software (v2.4) with the SEQUEST search engine using the UniProt *Saccharomyces cerevisiae* reference database (TaxonID=559292, V2017-10-25) plus sequences of the five target human chaperone proteins. Mass tolerances of the precursor ion and fragment ion were set at 10 ppm and 0.6 Da, respectively. Dynamic modifications on Methionine (oxidation, +15.995 Da), protein N-terminus (Acetyl, +42.011; Met-loss, -131.040; Met-loss-Acetyl, -89.030) and static modifications on Cysteine (carbamidomethyl, +57.021 Da) were allowed. Only peptides and proteins with high confidence (false discovery rate <1%) were reported.

Magic Marker complementation assay

Yeast heterozygous diploid deletion Magic Marker strains M.M. PBA1, M.M. PBA2, M.M. PBA3, M.M. PBA4, M.M. UMP1 strains [38] were transformed with expression vectors containing orthologous human chaperone genes. After two days of incubation at 30°C on selection medium (SD-URA), a single survivor colony was streaked out and grown on another SD-URA plate and growth overnight. Swaths of M.M. transformants were then transferred to liquid sporulation mix consisting of 1 ml 10% potassium acetate, 100 µl 0.5% zinc acetate, and 9 ml dH_2O within a 15 ml Falcon tube. Falcon tubes containing suspended M.M. strains were then rotated at room temperature for 72 hours in a benchtop RotoFlex. An optical microscope was used to confirm the presence of sporulated cells in the solution prior to spotting dilutions on M.M.-G418 and M.M.+G418 agar plates. After incubation at 30°C or 37°C, colonies were imaged to assess complementation. Results from M.M.-G418 are not shown because *pba1Δ, pba2Δ, pba3Δ, or pba4Δ* strains were all viable with no observable growth defects.

Growth rate assessment and analysis

Transformant strains were inoculated in 5ml SD-URA and grown overnight at 30˚C. 1µl of each seed culture was then added to 149µl SD-URA in a 96-well flat bottom, clear microplate (Corning #3595). Plates containing yeast cultures were then placed in SynergyH1 multimode microplate reader set to 30°C with continuous double orbital shaking at 280 rpm, and optical density (OD) at 595nm was measured at 20-minute intervals for 72 hours. Results growth curves were plotted using Prism software and doubling times were calculated by fitting background subtracted data to the equation: $Y = Y_0 e^{kt}$, where Y is yeast culture OD_{595nm} at a given time (t), Y_0 is culture OD_{595nm} at time = 0, and k is the growth constant. Doubling time (T) was then calculated using the equation: $T = \ln(2)/k$.

Generation and phenotyping of the *pba1*Δ*pba2*Δ double knockout mutant

SN3496 and dma3254 yeast strains (kind gifts from Elena Kuzmin, Concordia University) were mixed together, transferred to a YPD agar plate and grown overnight at 30°C to promote mating. Mixed yeast colonies were then streaked on YPD plates containing NAT and G418 and then incubated for 2 days at 30°C to obtain monoclonal diploid colonies, that were patched on agar plates containing sporulation medium and incubated for 7 to 10 days at 20°C. Sporulation was confirmed using light microscopy and single tetrad colonies were suspended in 100µl zymolyase solution (70µl dH_2O and 7.7µl 5mg/ml zymolyase in 1M sorbitol) followed by incubation at 37°C for 5 minutes. 500µl dH_2O was added to stop the zymolyase reaction, 20µl was spread linearly on a SC plate, and after drying, tetrad dissection was carried out using SporePlay+ dissection microscope. Separated spores were grown for 2 days at 30°C, then replica plated onto YPD, YPD+G418, YPD+NAT, TY2014 and TY2625 plates using fabric on block. These plates were then incubated for 2 days prior to being imaged. TY2014 and TY2625 strains for tetrad analysis were gifts from Elena Kuzmin (Concordia University). For each strain, 200µl of seed culture grown in YPD overnight at 30˚C was spread evenly on a YPD agar plate and then the plates were dried for 2 hours.

Construction of RPN11-GFP yeast strains

Genomic DNA was prepared from a BY4741 yeast strain containing GFP inserted behind RPN11 in the genome [57]. PCR amplification was carried out, using a forward primer specific to 247 bp upstream from the 3' end of RPN11 and a reverse primer specific to 209 bp downstream from the RPN11 3' end, to obtain a repair template that was verified by Oxford Nanopore sequencing (Plasmidsaurus) and transformed into humanized yeast strains of interest. Colonies that grew on SD-HIS media (presumably due to genomic integration of GFP-tag by homologous recombination) were selected and genotyped by PCR, using a forward primer targeting RPN11 region just upstream of the homologous region and a reverse primer targeting GFP, to ensure the GFP gene was integration correctly at the end of RPN11 **(Fig 9)**.

Fluorescence microscopy

Seed cultures of yeast strains were grown overnight at 30˚C in SC media and then used to inoculate fresh cultures grown to OD_{595nm} 0.6 or 1.5 on the day of the experiment. A Leica DMI 6000 inverted epifluorescence microscope (located in the Centre for Microscopy and Cellular Imaging at Concordia University) was used to image intracellular GFP localization, and captured micrographs were processed using FIJI software for presentation.

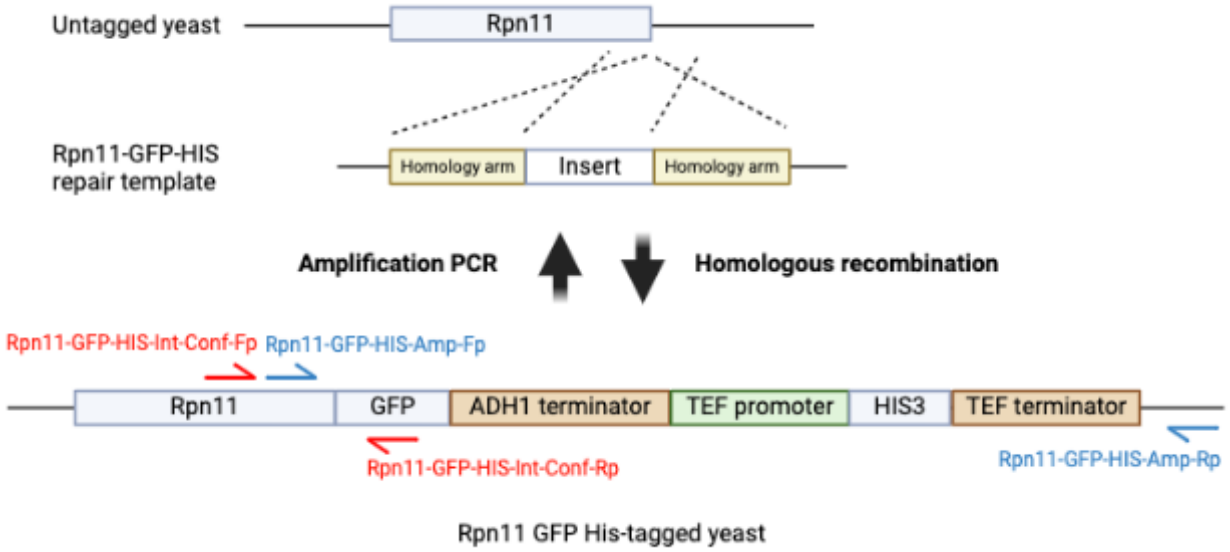

Figure 9. Genetic engineering strategy to introduce GFP-tag at 3' end of *RPN11*. Repair template with approximate homology arm of ~250 bp is amplified from Rpn11 GFP-His tagged yeast using amplification primers (blue). This repair template is transformed into untagged humanized yeast strains for homologous recombination, and confirmation primers (red) are used to check if GFP tag is correctly fused at the end of Rpn11.

Table 2. Primers used in this study

Name	Sequence
Rpn11-GFP-HIS-Amp-Fp	5'-AGAACAGTGGCAATCAGGTCT-3'
Rpn11-GFP-HIS-Amp-Rp	5'-TGGGAAAAGCAAGAGTGAAAGA-3'
Rpn11-GFP-His-Int-Conf-Fp	5'-ACCGCGAAGGAAACCAAGAT-3'
Rpn11-GFP-HIS-Int-Conf-Rp	5'-GCATCACCTTCACCCTCTCC-3'

Table 3. Yeast strains used in this study

Name	Genotype	Reference
BY4741 WT	***MATa*** *his3Δ1 leu2Δ0 met15Δ0 ura3Δ0*	[53]
BY4743 Magic Marker PBA1	BY4743; *MAT*a/α *PBA1/pba1*Δ::*kanMX* CAN1/*can1Δ*::LEU2-MFA1pr HIS3	[38]
BY4743 Magic Marker PBA2	BY4743; *MAT*a/α *PBA2/pba2*Δ::*kanMX* CAN1/*can1Δ*::LEU2-MFA1pr HIS3	[38]
BY4743 Magic Marker PBA3	BY4743; *MAT*a/α *PBA3/pba3*Δ::*kanMX* CAN1/*can1Δ*::LEU2-MFA1pr HIS3	[38]
BY4743 Magic Marker PBA4	BY4743; *MAT*a/α *PBA4/pba4*Δ::*kanMX* CAN1/*can1Δ*::LEU2-MFA1pr HIS3	[38]
BY4743 Magic Marker UMP1	BY4743; *MAT*a/α *UMP1/ump1*Δ::*kanMX* CAN1/*can1Δ*::LEU2-MFA1pr HIS3	[38]
SN3476	*YKL206C^NatR can1^::STE2pr-Sp_his5 lyp1^*	[54]
dma3254	*pba1^0::kanMX4 his3^1 leu2^0 ura3^0 met15^0*	[54]
TY2014	***MATα*** *ste3Δ306::LEU2 sst2 Δ ste2 Δ mfa1 Δ mfa2 Δ::FUS1-lacZFUS1::HIS3 ura3-52 leu2-3 112 ade1*	[54]
TY2625	***MATa*** *bar1 Δ his3::FUS1-HIS3 mfa2 Δ:: FUS1-lacZ ura3-1 leu2-3 -112 trp1-1 ade2-1 can1-100*	[54]
BY4741 *PBA1ΔPBA2Δ*	BY4741; *pba1^0::kanMX4 YKL206C^NatR*	This study
BY4741 *Hs*-α1	BY4741; *SCL1*Δ::Hs*PSMA6*	[24]
BY4741 *Hs*-α2	BY4741; *PRE8*Δ::Hs*PSMA2*	[24]
BY4741 *Hs*-α3	BY4741; *PRE9*Δ::Hs*PSMA4*	[24]
BY4741 *Hs*-α4	BY4741; *PRE6*Δ::Hs*PSMA7*	[24]
BY4741 *Hs*-α5	BY4741; *PUP2*Δ::Hs*PSMA5*	[24]
BY4741 *Hs*-α6	BY4741; *PUP3*Δ::Hs*PSMB3*	[24]
BY4741 *Hs*-α7	BY4741; *PUP3*Δ::Hs*PSMB3*	[24]

BY4741 *Hs*-α123	BY4741; *SCL1*Δ::Hs*PSMA6 PRE8*Δ::Hs*PSMA2 PRE9*Δ::Hs*PSMA4*	[24]
BY4741 *Hs*-β3	BY4741; *PUP3*Δ::Hs*PSMB3*	[24]
BY4741 *Hs*-β4	BY4741; *PRE1*Δ::Hs*PSMB2*	[24]
BY4741 *Hs*-β3β2	BY4741; *PUP1*Δ::Hs*PSMB7 PUP3*Δ::Hs*PSMB3*	[24]
BY4741 *Hs*-β2 S214G	BY4741; *PUP1*Δ::Hs*PSMB7*(S214G)	[27]
BY4741 *Hs*-α123467	BY4741; *SCL1*Δ::Hs*PSMA6 PRE8*Δ::Hs*PSMA2 PRE9*Δ::Hs*PSMA4 PRE6*Δ::Hs*PSMA7 PUP3*Δ::Hs*PSMB3 PUP3*Δ::Hs*PSMB3*	[24]
BY4741 *Hs*-α123467β3	BY4741; *SCL1*Δ::Hs*PSMA6 PRE8*Δ::Hs*PSMA2 PRE9*Δ::Hs*PSMA4 PRE6*Δ::Hs*PSMA7 PUP3*Δ::Hs*PSMB3 PUP3*Δ::Hs*PSMB3 PUP3*Δ::Hs*PSMB3*	[24]
BY4741 *Hs*-α467homo5het	BY4741; *PRE6*Δ::Hs*PSMA7 PUP3*Δ::Hs*PSMB3 PUP2*/Hs*PSMA5 PUP3*Δ::Hs*PSMB3*	[24]
WT Rpn11-GFP	BY4741; *RPN11*-3'tag-*GFP*(S65T)-*HIS3*	[55]
Hs-α1 Rpn11-GFP	BY4741 *Hs*-α1; *RPN11*-3'tag-*GFP*(S65T)-*HIS3*	This study
Hs-α2 Rpn11-GFP	BY4741 *Hs*-α2; *RPN11*-3'tag-*GFP*(S65T)-*HIS3*	This study
Hs-α3 Rpn11-GFP	BY4741 *Hs*-α3; *RPN11*-3'tag-*GFP*(S65T)-*HIS3*	This study
Hs-α4 Rpn11-GFP	BY4741 *Hs*-α4; *RPN11*-3'tag-*GFP*(S65T)-*HIS3*	This study
Hs-α5 Rpn11-GFP	BY4741 *Hs*-α5; *RPN11*-3'tag-*GFP*(S65T)-*HIS3*	This study
Hs-α6 Rpn11-GFP	BY4741 *Hs*-α6; *RPN11*-3'tag-*GFP*(S65T)-*HIS3*	This study
Hs-α7 Rpn11-GFP	BY4741 *Hs*-α7; *RPN11*-3'tag-*GFP*(S65T)-*HIS3*	This study
Hs-α123 Rpn11-GFP	BY4741 *Hs*-α123; *RPN11*-3'tag-*GFP*(S65T)-*HIS3*	This study

Table 4. Plasmids used in this study

Name	Reference
CEN6URA GFP	[24]
CEN6URA::PSMG1	This study
CEN6URA::PSMG2	This study
CEN6URA::PSMG3	This study
CEN6URA::PSMG4	This study
CEN6URA::POMP	This study
CEN6URA::PSMG12	This study
CEN6URA::PSMG34	This study
CEN6URA::PSMG1234	This study
CEN6URA::PSMG1234+POMP	This study
CEN6G418::PSMG1234+POMP	This study

Chapter 7: Bibliography

1. Milo, R. (2013). What is the total number of protein molecules per cell volume? A call to rethink some published values. *BioEssays* 35(12), 1050–1055.
2. McShane, E. *et al.* (2016) Kinetic Analysis of Protein Stability Reveals Age-Dependent Degradation. *Cell* 167(3), 583-870.
3. Jayaraj, G. G. *et al*. (2019). Functional modules of the proteostasis network. *Cold Spring Harbor Perspectives in Biology* 12(1), a033951.
4. Ryazanov, A. G., & Nefsky, B. S. (2002). Protein turnover plays a key role in aging. *Mechanisms of Ageing and Development* 123(2–3), 207–213.
5. Wang, S. S. *et al*. (2007). Diseases of protein aggregation and the hunt for potential pharmacological agents. *Biotechnology Journal* 3(2), 165–192.
6. Tanaka, K. (2009). The proteasome: Overview of structure and functions. *Proceedings of the Japan Academy Series B* 85(1), 12–36.
7. Saeki, Y., & Tanaka, K. (2007). Unlocking the proteasome door. *Molecular Cell* 27(6), 865–867.
8. Groll, M. *et al.* (1997). Structure of 20S proteasome from yeast at 2.4Å resolution. *Nature* 386(6624), 463–471.
9. Harris J. L. *et al.* (2001) Substrate specificity of the human proteasome. *Chemistry & Biology* 8(12), 1131-1141.
10. Köhler, A. *et al*. (2001). The axial channel of the proteasome core particle is gated by the RPT2 ATPASE and controls both substrate entry and product release. *Molecular Cell* 7(6), 1143–1152.
11. Paramonova, N. *et al*. (2021). Genetic variations in the PSMA6 and PSMC6 proteasome genes are associated with multiple sclerosis and response to interferon-β therapy in Latvians. *Experimental and Therapeutic Medicine* 21(5), 478.
12. Cao, Y. *et al*. (2020). Proteasome, a Promising Therapeutic Target for Multiple Diseases Beyond Cancer. *Drug Design Development and Therapy* 14, 4327–4342.
13. George, D. E., & Tepe, J. J. (2021). Advances in proteasome enhancement by small molecules. *Biomolecules* 11(12), 1789.
14. Leonardo-Sousa, C. *et al.* (2022). Revisiting Proteasome Inhibitors: Molecular Underpinnings of Their Development, Mechanisms of Resistance and Strategies to Overcome Anti-Cancer Drug Resistance. *Molecules* 27(7), 2201
15. Nakatogawa, H. *et al.* (2009). Dynamics and diversity in autophagy mechanisms: lessons from yeast. *Nature Reviews Molecular Cell Biology* 10(7), 458–467.

16. Varshavsky, A. (2006). The early history of the ubiquitin field. *Protein Science 15*(3), 647–654.

17. Xie, Y., & Varshavsky, A. (2001). RPN4 is a ligand, substrate, and transcriptional regulator of the 26S proteasome: A negative feedback circuit. *Proceedings of the National Academy of Sciences 98*(6), 3056–3061.

18. Kachroo, A. H. *et al.* (2022). Humanized yeast to model human biology, disease and evolution. *Disease Models & Mechanisms* 15(6), dmm049309.

19. Roohvand, F. *et al.* (2020). Biomedical applications of yeasts - a patent view, part two: era of humanized yeasts and expanded applications. *Expert Opinion on Therapeutic Patents* 30(8), 609–631.

20. Kachroo, A. H. *et al.* (2015). Systematic humanization of yeast genes reveals conserved functions and genetic modularity. *Science* 348(6237), 921–925.

21. Khurana, V., & Lindquist, S. (2010). Modelling neurodegeneration in Saccharomyces cerevisiae: why cook with baker's yeast? *Nature Reviews. Neuroscience*, *11*(6), 436–449

22. Dhakal, S., & Macreadie, I. (2020). Protein homeostasis networks and the use of yeast to guide interventions in Alzheimer's disease. *International Journal of Molecular Sciences* 21(21), 8014.

23. Kulagin, K. A. *et al*. (2024). Synergistic Effect of a Combination of Proteasome and Ribonucleotide Reductase Inhibitors in a Biochemical Model of the Yeast Saccharomyces cerevisiae and a Glioblastoma Cell Line. *International Journal of Molecular Sciences* 25(7), 3977.

24. Abdullah, M. *et al.* (2023). Rapid, scalable, combinatorial genome engineering by marker-less enrichment and recombination of genetically engineered loci in yeast. *Cell Reports Methods* 3(5), 100464.

25. Wagner, G. P. *et al*. (2007). The road to modularity. *Nature Reviews Genetics* 8(12), 921–931.

26. Chen, Y., & Dokholyan, N. V. (2006). The coordinated evolution of yeast proteins is constrained by functional modularity. *Trends in Genetics* 22(8), 416–419.

27. Sultana, S. *et al*. (2023). Species-specific protein–protein interactions govern the humanization of the 20S proteasome in yeast. *Genetics* 225(1), iyad117.

28. Morris, E. P., & Da Fonseca, P. C. A. (2021). How to build a proteasome. *Nature Structural & Molecular Biology* 28(5), 409–410.

29. Adolf, F. *et al*. (2024). Visualizing chaperone-mediated multistep assembly of the human 20S proteasome. *Nature Structural & Molecular Biology* 31(8), 1176–1188.

30. Matias, A. C. *et al*. (2022). HSP70 and HSP110 chaperones promote early steps of proteasome assembly. *Biomolecules* 13(1), 11.

31. Song, C. *et al.* (2021). Structural Fluctuations of the Human Proteasome α7 Homo-Tetradecamer Double Ring Imply the Proteasomal α-Ring Assembly Mechanism. *International Journal of Molecular Sciences* 22(9), 4519.

32. Wu, W. *et al.* (2018). PAC1-PAC2 proteasome assembly chaperone retains the core α4-α7 assembly intermediates in the cytoplasm. *Genes to Cells* 23(10), 839–848.

33. Hirano, Y. *et al.* (2008). Dissecting β-ring assembly pathway of the mammalian 20S proteasome. *The EMBO Journal* 27(16), 2204–2213.

34. Rousseau, A., & Bertolotti, A. (2018). Regulation of proteasome assembly and activity in health and disease. *Nature Reviews Molecular Cell Biology* 19(11), 697–712.

35. Li, X. *et al.* (2007). β-Subunit appendages promote 20S proteasome assembly by overcoming an Ump1-dependent checkpoint. *The EMBO Journal* 26(9), 2339–2349.

36. Sasaki, K. *et al.* (2010). PAC1 gene knockout reveals an essential role of Chaperone-Mediated 20S proteasome biogenesis and latent 20S proteasomes in cellular homeostasis. *Molecular and Cellular Biology* 30(15), 3864–3874.

37. Fricke, B. *et al.* (2007). The proteasome maturation protein POMP facilitates major steps of 20S proteasome formation at the endoplasmic reticulum. *EMBO Reports* 8(12), 1170–1175.

38. Pan, X. *et al.* (2004). A robust toolkit for functional profiling of the yeast genome. *Molecular Cell* 16(3), 487–496.

39. Giaever, G. *et al.* (2002). Functional profiling of the Saccharomyces cerevisiae genome. Nature 418(6896), 387–391

40. Hilt, W., & Wolf, D. H. (1992). Stress-induced proteolysis in yeast. *Molecular Microbiology* 6(17), 2437–2442

41. Xie, Z. *et al.* (2024). Proteasome resides in and dismantles plant heat stress granules constitutively. *Molecular Cell* 84(17), 3320-3335.e7

42. Enenkel, C. *et al.* (2022). Intracellular localization of the proteasome in response to stress conditions. *Journal of Biological Chemistry* 298(7), 102083.

43. Wendler, P., & Enenkel, C. (2019). Nuclear transport of yeast proteasomes. *Frontiers in Molecular Biosciences* 6.

44. De Almeida, M. *et al.* (2021). AKIRIN2 controls the nuclear import of proteasomes in vertebrates. *Nature* 599(7885), 491–496.

45. Hirayama, S. *et al.* (2018). Nuclear export of ubiquitinated proteins via the UBIN-POST system. *Proceedings of the National Academy of Sciences* 115(18), 4199-4208.

46. Park, S. *et al.* (2013). PolyQ Proteins Interfere with Nuclear Degradation of Cytosolic Proteins by Sequestering the Sis1p Chaperone. *Cell* 154(1), 134–145.

47. Miller, S. B. *et al.* (2015). Compartment-specific aggregases direct distinct nuclear and cytoplasmic aggregate deposition. *The EMBO Journal* 34(6), 778–797.

48. Lehmann, A. *et al.* (2002). 20 S proteasomes are imported as precursor complexes into the nucleus of yeast. *Journal of Molecular Biology* 317(3), 401–413.

49. Waite, K. A. *et al.* (2020). Tagging the proteasome active site β5 causes tag specific phenotypes in yeast. *Scientific Reports* 10(1), 18133.

50. Akhmetov, A. (2019). *Yeast as a platform for synthetic biology and investigation of evolutionary hypotheses* [Doctoral dissertation, University of Texas at Austin]. Texas ScholarWorks. http://dx.doi.org/10.26153/tsw/2162

51. Vandeloo, M. (2022). *Humanization of the sterol biosynthesis pathway in yeast* [Master's thesis, Concordia University]. Spectrum Research Repository. https://spectrum.library.concordia.ca/id/eprint/991451/

52. Lee, M. E. *et al.* (2015). A highly characterized Yeast toolkit for modular, multipart assembly. *ACS Synthetic Biology* 4(9), 975–986.

53. Brachmann, C.B. *et al.* (1998). Designer deletion strains derived from Saccharomyces cerevisiae S288C: a useful set of strains and plasmids for PCR-mediated gene disruption and other applications. *Yeast*, 14(2), 115-32.

54. Kuzmin, E. (2016). *Revealing Retention Mechanisms of Duplicated Genes and Surveying Triple Mutant Genetic Interaction Space in Yeast* [Doctoral dissertation, University of Toronto]. TSpace. http://hdl.handle.net/1807/77860

55. Huh, W. *et al.* (2003). Global analysis of protein localization in budding yeast. *Nature* 425(6959), 686–691.